

Direct Measurement of Higher-Order Nonlinear Polarization Squeezing

Nidhin Prasannan,¹ Jan Sperling,² Benjamin Brecht,¹ and Christine Silberhorn¹

¹*Integrated Quantum Optics Group, Institute for Photonic Quantum Systems (PhoQS), Paderborn University, Warburger Straße 100, 33098 Paderborn, Germany*

²*Theoretical Quantum Science, Institute for Photonic Quantum Systems (PhoQS), Paderborn University, Warburger Straße 100, 33098 Paderborn, Germany*

(Dated: April 15, 2022)

We report on nonlinear squeezing effects of polarization states of light by harnessing the intrinsic correlations from a polarization-entangled light source and click-counting measurements. To quantify these quantum effects, we derive theoretical bounds for second- and higher-order moments of nonlinear quantum Stokes operators, described in two polarization modes. The experimental validation of our concept is rendered possible by developing an efficient source, which uses a spectrally decorrelated type-II phase-matched waveguide inside a Sagnac interferometer. Correlated click statistics and high-order moments are directly obtained from an eight-time-bin quasi-photon-number-resolving detection system. The generated macroscopic Bell states that are readily available with our source show the distinct nature of nonlinear polarization squeezing in up to eighth-order correlations, also matching our theoretical predictions. Furthermore, our data certifies nonclassical correlations with high statistical significance, without the need to correct for experimental imperfections and limitations.

Introduction.— Squeezing plays a vital role as a fundamental quantum effect and fosters today’s development of quantum technology. Because of this importance, squeezed states of light are studied on various physical platforms [1–5], harnessing their nonclassical properties to advance the performance of quantum imaging, sensing, and information processing applications [6–11]. Among the different ways squeezing can manifest itself, spin and polarization squeezed states of light are of particular interest [12–15].

In classical (statistical) optics, polarization properties are explained via Stokes parameters, frequently visualized on the Poincaré sphere. For quantum states of polarized light, the operator counterpart to Stokes parameters have been established [16]. Similar to squeezing in phase space, accessible via quadrature (i.e., field) operators, the idea here is to assess squeezing effects in terms of Stokes operator fluctuations [17]. Different theoretical techniques to quantify spin squeezing were proposed [18, 19], and a number of experiments have been performed where one looks at the quadrature and intensity uncertainties in different polarisation bases [20, 21].

Experiments often employ second-order moments for testing their results with respect to quantum-classical boundaries, not appreciating the information content provided by higher-order correlations; see, e.g., Ref. [22] for one exception. For quadrature squeezing, higher-order effects have been considered [23, 24]. Indeed, for characterizing the quantum polarization features of light, it was shown that higher-order polarization properties are essential [25]. In addition, and beyond the linear regime, it is exceedingly interesting from a fundamental point of view to study nonlinear quantum phenomena that are inaccessible via simple linear functional dependencies alone. However, higher-order and nonlinear quantum effects are hard to detect at best and often simply unattainable, restricting fundamental investigations and practical applications.

In general, the detection of complexly structured quantum light is experimentally challenging. In particular, phase-sensitive measurements typically require a well-defined, ex-

ternal reference phase, such as provided by the local oscillator in balanced homodyne detection [26]. For polarization measurements, interference properties of the two polarisation components suffice to characterize the quantum state [16, 17]. Still, such schemes commonly require photon-number-resolution capabilities, which are generally not available. Consequently, pseudo-number-resolving detection has been established to mitigate such limitations [27–30]. Using the therefore developed click-counting framework [31], it was shown that moment-based criteria allow for detecting nonclassical features with such incomplete photon-number information in theory [32] and experiment [33]. Nowadays, large detectors of up to 128 time-bin-multiplexed detectors are available, allowing us to explore even macroscopic quantum correlations [34]. While first theoretical attempts were made to combine click counting with problems pertaining to nonclassical polarization states [35], a full theoretical description and an experimental demonstration were not realized to date.

In addition to the detection, polarization-entangled sources based on parametric down-conversion have been successfully investigated [36, 37]. Yet, often these experiments solely exploit single-photon components to produce entangled Bell states and GHZ states [38] in a low-pump-power approximation. Intrinsically, however, the down-conversion process also leads to higher-order contributions. The full expansion for both polarizations yields a macroscopic Bell state [39], i.e., a continuous-variable Einstein–Podolski–Rosen state, whose quantum noise properties have been characterized in terms of second-order, linear Stokes-operator fluctuations [40]. But, specifically, the nonlinear functional dependencies of the resulting quantum correlations have not yet been explored.

In this contribution, we develop a nonlinear Stokes-operators formalism in terms of click-counting measurements. Based on this approach, second- and higher-order moment-based inequalities are derived that, when violated, certify nonclassical polarization states of quantum light. We combine an efficient source of entangled light with a click-counting de-

tection unit for the experimental verification of the nonclassicality. A parametric down-conversion source in a Sagnac loop [41] allows us to produce macroscopic Bell states with higher-order photon-number contributions and different polarization features, including complete and partial polarization nonclassicality. From the recorded time-multiplexed click pattern, we then directly reconstruct up to eighth-order moments for nonlinear Stokes operators, allowing us to characterize nonlinear quantum polarization effects with high statistical significance and without corrections for measurement imperfections.

Theory.— We employ a detection scheme in which incident light is split into $N = 8$ bins of equal intensity, each measured with a single-photon detector [27–30]. It was shown that obtaining k non-vacuum signals, i.e., clicks, is described by a positive operator-valued measure that exhibits a binomial form in a normally ordered expansion, $\hat{\Pi}_k = :(\hat{N})^k(\hat{1} - \hat{\pi})^{N-k}:$ [31], with $\hat{\pi} = \hat{1} - : \exp(-\eta \hat{n}/N) :$, where η , \hat{n} , and $: \dots :$ are the detection efficiency, the photon-number operator, and the normal order symbol, respectively. Importantly, this click-counting description is different from the common Poisson form for a full photon-number resolution, $\hat{\Pi}_k = :e^{-\eta \hat{n}}(\eta \hat{n})^k/k!:+ \mathcal{O}(1/N)$, with a rather slow $1/N$ convergence toward the photoelectric Poisson model [31]. Because of that, for example, equating a click with a photodetection event actually requires $N = 100$ detectors for a systematic error $\sim 1/N = 1\%$. Here, we directly work in the click-counting picture, not requiring corrections and utilizing the truly measured statistics.

For the two quantized polarization components, the linear representation is given in terms of Stokes operators. (See, e.g., Refs. [42, 43] for introductions.) That is, a wave-plate-based transformation of, say, horizontal and vertical photon numbers results in $\hat{a}^\dagger \hat{a} \mapsto (\hat{S}_0 + \mathbf{e} \cdot \hat{\mathbf{S}})/2$ and $\hat{b}^\dagger \hat{b} \mapsto (\hat{S}_0 - \mathbf{e} \cdot \hat{\mathbf{S}})/2$, respectively. Therein, the Stokes-operator vector is given by $\hat{\mathbf{S}} = (\hat{a}^\dagger \hat{b} + \hat{b}^\dagger \hat{a}, -i\hat{a}^\dagger \hat{b} + i\hat{b}^\dagger \hat{a}, \hat{a}^\dagger \hat{a} - \hat{b}^\dagger \hat{b})$, the total photon number reads $\hat{S}_0 = \hat{a}^\dagger \hat{a} + \hat{b}^\dagger \hat{b}$, and the vector $\mathbf{e} = (\sin \vartheta \cos \varphi, \sin \vartheta \sin \varphi, \cos \vartheta)$ corresponds to the measurement projection direction on the polarization Poincaré sphere. For the applied combination of quarter- and half-wave plates, the relative phase is $\varphi = \arg(\rho^* \tau) \in [0, 2\pi]$, the transmission coefficient is $|\tau| = \cos \vartheta/2$ ($0 \leq \vartheta \leq \pi$), and the reflection coefficient is $|\rho| = \sin \vartheta/2$.

In our scenario, the mean click number for the two polarizations is $\langle N\hat{\pi}_A \rangle = N(1 - \langle : \exp[-\eta(\hat{S}_0 + \mathbf{e} \cdot \hat{\mathbf{S}})/(2N)] : \rangle)$ and $\langle N\hat{\pi}_B \rangle = N(1 - \langle : \exp[-\eta(\hat{S}_0 - \mathbf{e} \cdot \hat{\mathbf{S}})/(2N)] : \rangle)$ [32, 35]. To characterize the polarization state, one typically utilizes the difference photon number, $\hat{a}^\dagger \hat{a} - \hat{b}^\dagger \hat{b} \mapsto \mathbf{e} \cdot \hat{\mathbf{S}}$, resembling a detection on Poincaré sphere along \mathbf{e} . Analogously, we here consider the difference of clicks which is given by the expectation value of

$$\hat{S}_{\text{NL}} = N\hat{\pi}_A - N\hat{\pi}_B = 2N : \exp\left(-\frac{\eta}{2N}\hat{S}_0\right) \sinh\left(\frac{\eta}{2N}\mathbf{e} \cdot \hat{\mathbf{S}}\right) : \quad (1)$$

This operator is a nonlinear function of Stokes operators which includes a hyperbolic sine of the sought-after projection $\mathbf{e} \cdot \hat{\mathbf{S}}$, and which also includes an exponential scaling with

the total photon number, accounting for detector saturation of click-counting devices. Please note that the limit $N \rightarrow \infty$ yields $\hat{S}_{\text{NL}} = \eta e \cdot \hat{\mathbf{S}} + \mathcal{O}(1/N)$, and the general form of Eq. (1) resembles the balanced homodyne detection scenario for a single optical mode using the click-counting theory [44]. Similarly to the difference, the total (i.e., summed) click-number operator, mirroring the total photon number, reads

$$\begin{aligned} \hat{S}_{0,\text{NL}} &= N\hat{\pi}_A + N\hat{\pi}_B \\ &= 2N \left[\hat{1} - : \exp\left(-\frac{\eta}{2N}\hat{S}_0\right) \cosh\left(\frac{\eta}{2N}\mathbf{e} \cdot \hat{\mathbf{S}}\right) : \right] \end{aligned} \quad (2)$$

and additionally depends on $\mathbf{e} \cdot \hat{\mathbf{S}}$, contrasting the linear total photon number \hat{S}_0 without similar contributions; see Ref. [45] for analogous considerations for homodyne detection.

For determining polarization nonclassicality, we can now use the method of normally ordered matrices of moments [46, 47], which is adopted here for the derived nonlinear Stokes operators that are obtained through click-counting measurements. The resulting matrix $M = (\langle : \hat{S}_{\text{NL}}^{k+l} : \rangle)_{k,l=0,\dots,N/2}$ includes moments up to the N th order and is positive semidefinite for classical light, $M \geq 0$ [32]. If, however, $M \geq 0$ does not apply, nonclassicality is certified. As one example, we can consider the determinant of the principal leading two-dimensional submatrix of M . Then, this second-order, classical constraint reads

$$0 \leq \det \begin{pmatrix} \langle : \hat{S}_{\text{NL}}^0 : \rangle & \langle : \hat{S}_{\text{NL}}^1 : \rangle \\ \langle : \hat{S}_{\text{NL}}^1 : \rangle & \langle : \hat{S}_{\text{NL}}^2 : \rangle \end{pmatrix} = \langle : (\Delta \hat{S}_{\text{NL}})^2 : \rangle, \quad (3)$$

with $\langle : \hat{S}_{\text{NL}}^0 : \rangle = \langle \hat{1} \rangle = 1$, which lower-bounds the normally ordered and nonlinear variance of \hat{S}_{NL} for classical polarization states by zero. In this context, it is worth mentioning that the elements of M can be directly expressed in terms of moments of $\hat{\pi}_A$ and $\hat{\pi}_B$ through Eq. (1) which we obtain from $\langle : \hat{\pi}_A^j \hat{\pi}_B^{j'} : \rangle = \sum_{k=j}^N \sum_{l=j'}^N c_{k,l} \binom{k}{j} \binom{l}{j'} \binom{N}{j}^{-1} \binom{N}{j'}^{-1}$ [33], only and directly utilizing the actually measured joint click-counting statistics $c_{k,l}$ for both polarizations.

Experiment.— See Fig. 1(a) for the setup and Fig. 1(b) for the time-multiplexed click detection.

A periodically poled potassium titanyl phosphate (PPKTP) waveguide is operated inside a Sagnac interferometer [41]. Bidirectional pumping efficiently generates type-II parametric down-conversion in clockwise and counterclockwise propagation direction with non-negligible higher-order contributions. The pump light is delivered from a pulsed laser with 100 fs pulse duration and 774 nm central wavelength. A folded 4f spectrometer is used to select a narrow part of the pump spectrum, yielding pump pulses with 1 ps duration. Our engineered waveguide source generates spectrally decorrelated photon pairs independently and probabilistically in both directions. A HWP at a fixed angle, 45° , inside the interferometer switches the polarization, ensuring that pump and down-converted (i.e., signal and idler) photons have identical polarization when they recombine on the Sagnac PBS. Interfering the resulting beams on the Sagnac PBS generates entangled

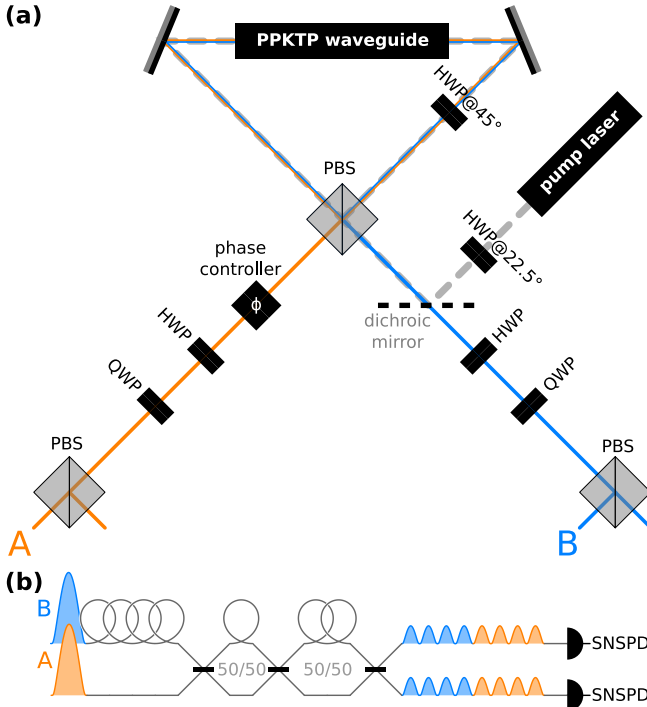


FIG. 1. Setup outline. A 775 nm laser pumps the waveguide source with a spectrally filtered pump width of 1 ps. Polarization-entangled photon pairs are generated in the forward and backward propagation in the Sagnac interferometer and separated with a polarizing beam splitter (PBS). A phase controller allows to switch between symmetric and anti-symmetric Bell states, as discussed later. Combinations of half- and quarter-wave plates (HWP and QWP, respectively) with a PBS yield arbitrary Stokes projections $e \cdot \hat{S}$ on the Poincaré sphere. Our time-multiplexed detector (TMD) is built from low-loss fibers and 50/50 beam splitters. The resulting time-bin-resolved photons in arms *A* and *B* are detected by two superconducting nanowire single-photon detectors (SNSPDs) with an efficiency $> 80\%$.

light in two output modes. The source performance is benchmarked with a visibility of $> 96\%$ and a fidelity of $> 95\%$ in the low-pump-power regime. The phase in arm *A* is tuned with a 1550 nm Soleil–Babinet compensator, labeled as phase controller in Fig. 1(a). HWP and QWP combinations are used to perform arbitrary Stokes measurements. The measurement PBSs project the light state into the two polarization modes and direct beams *A* and *B* to our detection unit.

For click counting, the produced entangled light is sent through an eight-time-bin detection unit, Fig. 1(b). Our TMD consists of a series of three 50/50 beam splitters connected by delay fibers with different lengths, resulting in a splitting of the input signal into different time bins [28, 29]. Time bins are separated by 100 ns. Since two light beams *A* and *B* are coming from the setup, both inputs of one TMD can be utilized in a delayed manner, allowing for a resource-efficient characterization of quantum light. A total of 16 time-bins for *A* and *B* are then detected by two SNSPDs, which have dead time of 60 ns, much less than the bin separation. The repetition rate of the experiment is reduced to 1 MHz to account for

the time delays introduced by the TMD detection scheme.

Results.— Relatively strong pumping (here, 100 μW , or 0.1 nJ per pulse) of the nonlinear source sandwiched in Sagnac interferometer produces polarization-entangled states with higher-order photon-number contributions. Our waveguide-based approach benefits from a high degree of spatial light confinement and thus produces bright quantum light, not being limited as bulk-crystal-based sources that suffer spatial distortions, such as Kerr lensing. The produced state after the phase controller takes the form

$$|\psi\rangle = (1 - |\lambda|^2) \sum_{m,n=0}^{\infty} \lambda^m (e^{i\phi} \lambda)^n |m\rangle \otimes |n\rangle \otimes |n\rangle \otimes |m\rangle, \quad (4)$$

with $|\lambda| < 1$; the tensor products of number states are sorted according to output arm and polarization as follows: horizontal for *A*, vertical for *A*, horizontal for *B*, and vertical for *B*. We specifically use the controller settings $e^{i\phi} = \pm 1$, defining macroscopic Bell states $|\psi_{\pm}\rangle$ [40]. That name for the continuous-variable state in Eq. (4) originates from the two-photon subspace (i.e., $m + n = 1$) in which we have an entangled two-qubit state—meaning that we can write in that case $|\psi\rangle \sim |H\rangle \otimes |V\rangle + e^{i\phi} |V\rangle \otimes |H\rangle$ for modes *A* and *B*, with the horizontal and vertical single-photon states $|H\rangle = |1\rangle \otimes |0\rangle$ and $|V\rangle = |0\rangle \otimes |1\rangle$, respectively. (Please note the symmetric and anti-symmetric exchange symmetry between *A* and *B* for $e^{i\phi} = \pm 1$.) By controlling the squeezing strength via λ , one thus obtains entangled qubit and qudit states in the two-photon and few-photon regime (where $|\lambda| \approx 0$) and macroscopic Bell states for high pump powers, i.e., higher $|\lambda|$ values.

Using a polarization tomography, including HWPs, QWPs, and PBSs, in both modes, we collect data for 1300 s, resulting in ca. 10^8 events with different coincidence counts k and l for *A* and *B*, respectively, yielding the joint click-counting statistics $c_{k,l}$ for each waveplate setting and state $|\psi_{\pm}\rangle$. For the sake of exhibition, we vary either HWP or QWP angles, while keeping the other waveplate at 0° and using the same angles for both *A* and *B*.

From this data, we can directly infer the nonlinear Stokes-parameter fluctuations, Eq. (3), that are depicted in the top row of Fig. 2. Via the highly significant negativities, nonlinear polarization squeezing is observed for the generated macroscopic Bell states; please note that a 15-standard-deviation uncertainty is depicted in all plots in Fig. 2.

Our theoretical model (dashed lines in Fig. 2) is based on our click-counting description in the theory part and the macroscopic Bell states in Eq. (4). Importantly, for all depicted scenarios, we use a single set of only two fit parameters to compare theory and experiment. That is, the overall efficiency of our setup is estimated as $\eta = 13.5\%$, and we have a relatively high $\lambda = 0.360$ —corresponding to 3.3 dB quadrature squeezing—that parametrizes both states $|\psi_{\pm}\rangle$ for all waveplate settings. (Recall that $|\lambda| \in [0, 1[$, meaning that 0.360 is clearly not close to zero.) Small experiment-theory deviations originate from slightly fluctuating pump powers over the experimental run, and the theoretical assumption that

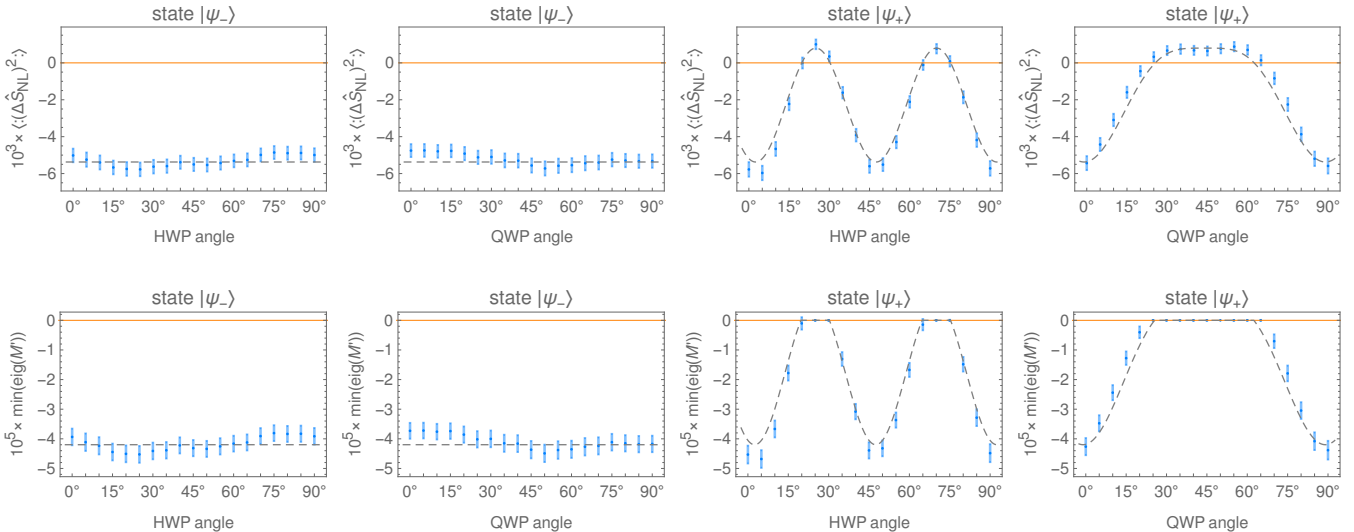


FIG. 2. Second-order and higher-order nonlinear polarization nonclassicality are depicted as negativities in the top and bottom row of plots, respectively. The first column of plots shows the results for the symmetric macroscopic Bell state in Eq. (4) for $\phi = 0$ as a function of the QWP angle and a fixed HWP angle at zero degree, and vice versa for the second column. The third and fourth column include analogous findings for the anti-symmetric macroscopic Bell state, $\phi = \pi$. A $\pm 15\sigma$ error margin is provided as a vertical bar. The theoretical model is shown as dashed lines in all plots for the single set of fit parameters $\lambda = 0.36$ and $\eta = 0.135$.

all polarizations and polarization-altering components are perfectly aligned.

Thus far, we demonstrated a nonlinear, yet second-order nonclassical polarization in terms of inequality (3). Previously, we also outlined that, with $N = 8$ detection bins, a normally ordered matrix of up to eighth-order moments of \hat{S}_{NL} can be used. In addition, the total click number $\hat{S}_{0,NL}$ was shown to be polarization-dependent in click-counting scenarios, too; see the contribution that includes $\mathbf{e} \cdot \hat{\mathbf{S}}$ in Eq. (2). Hence, we can use those information in terms of moments $\hat{S}_{0,NL}^m$: (for $m = 0, \dots, N$) for our purposes as well. Moreover, because of relations (1) and (2), a bijection exists to moments of $\hat{\pi}_A$ and $\hat{\pi}_B$, which is $\hat{\pi}_A = (\hat{S}_{0,NL} + \hat{S}_{NL})/N$ and $\hat{\pi}_B = (\hat{S}_{0,NL} - \hat{S}_{NL})/N$. Thus, we can equally use the matrix

$$M' = (\langle : \hat{\pi}_A^{j_A} \hat{\pi}_B^{j_B} : \rangle)_{(j_A, j_B), (j'_A, j'_B) \in \{0, \dots, N/2\} \times \{0, \dots, N/2\}}, \quad (5)$$

where rows and columns are defined through index pairs $(j_A^{(i)}, j_B^{(i)})$, for our higher-order nonclassicality analysis. (See Refs. [32, 33, 45] for additional details.) That is, if the minimal eigenvalue of M' is below zero, $\min(\text{eig}(M')) < 0$, we infer nonlinear polarization nonclassicality by using up to the eighth-order moments for both $\hat{S}_{0,NL}$ and \hat{S}_{NL} , being the maximal information contents extractable from a two-mode click-counting measurement with $N = 8$ detection bins [32, 35]. Consequently, we are not limited to second-order moments and can explore other nonclassical statistical signatures in the skewness (third order), kurtosis (fourth order), etc. In addition, we simultaneously find a useful meaning of the phase-sensitive total click number when determining quantum correlations in arbitrary polarization bases.

The bottom row in Fig. 2 shows the results for our data

for macroscopic Bell states $|\psi_{\pm}\rangle$. In any polarization setting, $|\psi_-\rangle$ shows a higher-order, nonlinear polarization well below the classical bound of zero. On the other hand, for $|\psi_+\rangle$, such nonclassical correlations depend on the waveplate settings. In comparison with the second-order approach, however, the higher-order moments never rise above the classical-quantum boundary at zero. Again, all higher-order nonclassical polarization effects are certified with high statistical significance and agree with our theoretical prediction.

Conclusion.— We devised a theoretical approach for a nonlinear Stokes-operator framework that is directly accessible via state-of-the-art click-counting measurements. In addition, we derived criteria that render it possible to detect nonclassical polarization states of light in this manner. Furthermore, we implemented this approach, experimentally demonstrating nonlinear polarization squeezing and even higher-order nonclassical signatures. To this end, macroscopic Bell states were generated via a waveguide-based Sagnac source and measured using a single eight-bin click-counting detection unit for both polarizations. In contrast to measurements with true photon-number-resolving detectors, the total click number is also polarization dependent. We exploited this fact to certify nonlinear and nonclassical polarization by jointly using up to eighth-order moments for both nonlinear Stokes operators and total click number. All observed quantum signatures are in agreement with our theoretical model and are reported with high statistical significance and without requiring correction for imperfections, such as unavoidable losses, detector saturation, and incomplete photon-number resolution, all of which are included in the here-developed theory.

Therefore, we formulated and implemented a previously

unknown and easily accessible method to characterize the quantum nature of polarization states of light. This newfound potential can be harnessed in photonic quantum-enhanced applications, breaking classical bounds of what is achievable with classical and linear polarizations, ranging from qubits and qudits (i.e., few-photon states) all the way to macroscopic (i.e., continuous-variable) correlations.

Acknowledgments.— The authors thank Michael Stefszky for valuable comments. The Integrated Quantum Optics group acknowledges financial support through the European Commission through the H2020-FETFLAG-2018-03 project PhoG (Grant No. 820365) and the ERC project QuPoPCoRN (Grant No. 725366). J. S. acknowledges financial support from the Deutsche Forschungsgemeinschaft (DFG, German Research Foundation) through the Collaborative Research Center TRR 142 (Project No. 231447078, project C10).

[1] R. E. Slusher, L. W. Hollberg, B. Yurke, J. C. Mertz, and J. F. Valley, Observation of Squeezed States Generated by Four-Wave Mixing in an Optical Cavity, *Phys. Rev. Lett.* **55**, 2409 (1985).

[2] L. Wu, H. J. Kimble, J. L. Hall, and H. Wu, Generation of Squeezed States by Parametric Down Conversion, *Phys. Rev. Lett.* **57**, 2520 (1986).

[3] K. Hirosawa, H. Furumochi, A. Tada, F. Kannari, M. Takeoka, and M. Sasaki, Photon Number Squeezing of Ultrabroadband Laser Pulses Generated by Microstructure Fibers, *Phys. Rev. Lett.* **94**, 203601 (2005).

[4] M. Fiorentino, J. E. Sharping, P. Kumar, A. Porzio, and R. S. Windeler, Soliton squeezing in microstructure fiber, *Opt. Lett.* **27**, 649 (2002).

[5] P. Grangier, R. E. Slusher, B. Yurke, and A. LaPorta, Squeezed-light-enhanced polarization interferometer, *Phys. Rev. Lett.* **59**, 2153 (1987).

[6] E. S. Polzik, J. Carri, and H. J. Kimble, Spectroscopy with squeezed light, *Phys. Rev. Lett.* **68**, 3020 (1992).

[7] B. P. Abbott, *et al.* (LIGO Scientific Collaboration and Virgo Collaboration), Observation of Gravitational Waves from a Binary Black Hole Merger, *Phys. Rev. Lett.* **116**, 061102 (2016).

[8] J. Aasi, *et al.*, Enhanced sensitivity of the LIGO gravitational wave detector by using squeezed states of light, *Nat. Photonics* **7**, 613 (2013).

[9] M. Hillery, Quantum cryptography with squeezed states, *Phys. Rev. A* **61**, 022309 (2000).

[10] H. Vahlbruch, M. Mehmet, K. Danzmann, and R. Schnabel, Detection of 15 dB Squeezed States of Light and their Application for the Absolute Calibration of Photoelectric Quantum Efficiency, *Phys. Rev. Lett.* **117**, 110801 (2016).

[11] M. A. Taylor, J. Janousek, V. Daria, J. Knittel, B. Hage, H.-A. Bachor, and W. P. Bowen, Biological measurement beyond the quantum limit, *Nat. Photonics* **7**, 229 (2013).

[12] F. Wolfgramm, A. Cerè, F. A. Beduini, A. Predojević, M. Koschorreck, and M. W. Mitchell, Squeezed-Light Optical Magnetometry, *Phys. Rev. Lett.* **105**, 053601 (2010).

[13] T. Horrom, R. Singh, J. P. Dowling, and E. E. Mikhailov, Quantum-enhanced magnetometer with low-frequency squeezing, *Phys. Rev. A* **86**, 023803 (2012).

[14] V. G. Lucivero, R. Jiménez-Martínez, J. Kong, and M. W. Mitchell, Squeezed-light spin noise spectroscopy, *Phys. Rev. A* **93**, 053802 (2016).

[15] L. Bai, L. Zhang, Y. Yang, R. Chang, Y. Qin, J. He, X. Wen, and J. Wang, Enhancement of spin noise spectroscopy of rubidium atomic ensemble by using the polarization squeezed light, *Opt. Express* **30**, 1925 (2022).

[16] A. Z. Goldberg, P. de la Hoz, G. Björk, A. B. Klimov, M. Grassl, G. Leuchs, and L. L. Sánchez-Soto, Quantum concepts in optical polarization, *Adv. Opt. Photonics* **13**, 1 (2021).

[17] G. S. Agarwal and S. Chaturvedi, Scheme to measure quantum stokes parameters and their fluctuations and correlations, *J. Mod. Opt.* **50**, 711 (2003).

[18] A. F. Abouraddy, A. V. Sergienko, B. E. A. Saleh, and M. C. Teich, Quantum entanglement and the two-photon Stokes parameters, *Opt. Commun.* **201**, 93 (2002).

[19] N. Korolkova, G. Leuchs, R. Loudon, T. C. Ralph, and C. Silberhorn, Polarization squeezing and continuous-variable polarization entanglement, *Phys. Rev. A* **65**, 052306 (2002).

[20] J. Heersink, V. Josse, G. Leuchs, and U. L. Andersen, Efficient polarization squeezing in optical fibers, *Opt. Lett.* **30**, 1192 (2005).

[21] W. P. Bowen, R. Schnabel, H.-A. Bachor, and P. K. Lam, Polarization Squeezing of Continuous Variable Stokes Parameters, *Phys. Rev. Lett.* **88**, 093601 (2002).

[22] M. Avenhaus, K. Laiho, M. V. Chekhova, and C. Silberhorn, Accessing Higher Order Correlations in Quantum Optical States by Time Multiplexing, *Phys. Rev. Lett.* **104**, 063602 (2010).

[23] C. K. Hong and L. Mandel, Higher-Order Squeezing of a Quantum Field, *Phys. Rev. Lett.* **54**, 323 (1985).

[24] M. Hillery, Amplitude-squared squeezing of the electromagnetic field, *Phys. Rev. A* **36**, 3796 (1987).

[25] J. Söderholm, G. Björk, A. B. Klimov, L. L. Sánchez-Soto, and G. Leuchs, Quantum polarization characterization and tomography, *New J. Phys.* **14**, 115014 (2012).

[26] D. T. Smithey, M. Beck, M. G. Raymer, and A. Faridani, Measurement of the Wigner distribution and the density matrix of a light mode using optical homodyne tomography: Application to squeezed states and the vacuum, *Phys. Rev. Lett.* **70**, 1244 (1993).

[27] H. Paul, P. Törmä, T. Kiss, and I. Jex, Photon Chopping: New Way to Measure the Quantum State of Light, *Phys. Rev. Lett.* **76**, 2464 (1996).

[28] D. Achilles, C. Silberhorn, C. Śliwa, K. Banaszek, and I. A. Walmsley, Fiber-assisted detection with photon number resolution, *Opt. Lett.* **28**, 2387 (2003).

[29] M. J. Fitch, B. C. Jacobs, T. B. Pittman, and J. D. Franson, Photon-number resolution using time-multiplexed single-photon detectors, *Phys. Rev. A* **68**, 043814 (2003).

[30] J.-L. Blanchet, F. Devaux, L. Furfarò, and E. Lantz, Measurement of Sub-Shot-Noise Correlations of Spatial Fluctuations in the Photon-Counting Regime, *Phys. Rev. Lett.* **101**, 233604 (2008).

[31] J. Sperling, W. Vogel, and G. S. Agarwal, True photocounting statistics of multiple on-off detectors, *Phys. Rev. A* **85**, 023820 (2012).

[32] J. Sperling, W. Vogel, and G. S. Agarwal, Correlation measurements with on-off detectors, *Phys. Rev. A* **88**, 043821 (2013).

[33] J. Sperling, M. Bohmann, W. Vogel, G. Harder, B. Brecht, V. Ansari, and C. Silberhorn, Uncovering Quantum Correlations with Time-Multiplexed Click Detection, *Phys. Rev. Lett.* **115**, 023601 (2015).

- [34] J. Tiedau, M. Engelkemeier, B. Brecht, J. Sperling, and C. Silberhorn, Statistical Benchmarking of Scalable Photonic Quantum Systems, *Phys. Rev. Lett.* **126**, 023601 (2021).
- [35] J. Sperling, W. Vogel, and G. S. Agarwal, Operational definition of quantum correlations of light, *Phys. Rev. A* **94**, 013833 (2016).
- [36] P. G. Kwiat, K. Mattle, H. Weinfurter, A. Zeilinger, A. V. Sergienko, and Y. Shih, New High-Intensity Source of Polarization-Entangled Photon Pairs, *Phys. Rev. Lett.* **75**, 4337 (1995).
- [37] M. M. Weston, H. M. Chrzanowski, S. Wollmann, A. Boston, J. Ho, L. K. Shalm, V. B. Verma, M. S. Allman, S. W. Nam, R. B. Patel, S. Slussarenko, and G. J. Pryde, Efficient and pure femtosecond-pulse-length source of polarization-entangled photons, *Opt. Express* **24**, 10869 (2016).
- [38] E. Meyer-Scott, N. Prasannan, I. Dhand, C. Eigner, V. Quiring, S. Barkhofen, B. Brecht, M. B. Plenio, and C. Silberhorn, Exponential enhancement of multi-photon entanglement rate via quantum interference buffering, [arXiv:1908.05722](https://arxiv.org/abs/1908.05722).
- [39] T. S. Iskhakov, I. N. Agafonov, M. V. Chekhova, and G. Leuchs, Polarization-Entangled Light Pulses of 10^5 Photons, *Phys. Rev. Lett.* **109**, 150502 (2012).
- [40] T. S. Iskhakov, M. V. Chekhova, G. O. Rytikov, and G. Leuchs, Macroscopic Pure State of Light Free of Polarization Noise, *Phys. Rev. Lett.* **106**, 113602 (2011).
- [41] E. Meyer-Scott, N. Prasannan, C. Eigner, V. Quiring, J. M. Donohue, S. Barkhofen, and C. Silberhorn, High-performance source of spectrally pure, polarization entangled photon pairs based on hybrid integrated-bulk optics, *Opt. Express* **26**, 32475 (2018).
- [42] S. Chaturvedi, G. Marmo, N. Mukunda, R. Simon, and A. Zampini, The Schwinger Representation of a Group: Concept and Applications, *Rev. Math. Phys.* **18**, 887 (2006).
- [43] G. Björk, J. Söderholm, L. L. Sánchez-Soto, A. B. Klimov, I. Ghiu, P. Marian, and T. A. Marian, Quantum degrees of polarization, *Opt. Commun.* **283**, 4440 (2010).
- [44] J. Sperling, W. Vogel, and G. S. Agarwal, Balanced homodyne detection with on-off detector systems: Observable nonclassicality criteria, *Europhys. Lett.* **109**, 34001 (2015).
- [45] T. Lipfert, J. Sperling, and W. Vogel, Homodyne detection with on-off detector systems, *Phys. Rev. A* **92**, 053835 (2015).
- [46] G. S. Agarwal and K. Tara, Nonclassical character of states exhibiting no squeezing or sub-Poissonian statistics, *Phys. Rev. A* **46**, 485 (1992).
- [47] E. Shchukin, T. Richter, and W. Vogel, Nonclassicality criteria in terms of moments, *Phys. Rev. A* **71**, 011802(R) (2005).